THE UNIVERSITY
OF QUEENSLAND

DEPARTMENT OF
CIVIL ENGINEERING
RESEARCH REPORT SERIES

Drag Reduction in Self-Aerated Flows. Analogy with Dilute Polymer Solutions and Sediment Laden Flows

H. CHANSON

Research Report No. CE141
October 1992

ISBN 0 86776 498 8

CIVIL ENGINEERING RESEARCH REPORTS

This report is one of a continuing series of Research Reports published by the Department of Civil Engineering at The University of Queensland. Lists of recently-published titles of this series and of other publications are provided inside the back cover of this report. Requests for copies of any of these documents should be addressed to the Departmental Secretary.

The interpretations and opinions expressed herein are solely those of the author(s). Considerable care has been taken to ensure the accuracy of the material presented. Nevertheless, responsibility for the use of this material rests with the user.

DEPARTMENT OF CIVIL ENGINEERING
THE UNIVERSITY OF QUEENSLAND
BRISBANE, AUSTRALIA 4072

Telephone:(07) 365 4163/4156 Telex: UNIVQLD AA40315
Fax: (07) 365 4599

DRAG REDUCTION IN SELF-AERATED FLOWS. ANALOGY WITH DILUTE POLYMER SOLUTIONS AND SEDIMENT LADEN FLOWS

by

H. CHANSON, M.E., ENSHMG, INSTN, Ph.D. (Cant.)

Lecturer in Civil Engineering

The University of Queensland

RESEARCH REPORT No. CE141

Department of Civil Engineering

The University of Queensland

October, 1992

Synopsis :

In supercritical open channel flows air is entrained at the free surface. Such air-water flows, called self-aerated flows, exhibit smaller friction losses than non-aerated flows. New data on drag reduction in self-aerated flows are presented. It is shown that the drag reduction process is linked with the presence of an air concentration boundary layer next to the channel bottom. An analogy with dilute polymer solutions and microbubble modified boundary layers is developed. It is suggested that the presence of air next to the bottom increases the effective viscosity of the mixture and the sublayer thickness.

A parallel with sediment laden flows is also developed. Although the distribution of suspended sediments differs from the distribution of air bubbles, it is suggested that the mechanisms of drag reduction observed in suspended sediment flows are similar to those in self-aerated flows.

Résumé :

Dans le cas d'écoulement à surface libre supercritiques, une certaine quantité d'air est entraînée à la surface libre. De tels écoulements à surface libre avec entraînement d'air sont caractérisés par des pertes de charge plus faibles. On présente de nouveaux résultats décrivant cette réduction du coefficient de perte de charge. L'auteur montre que le mécanisme de réduction des forces de frottement est lié à la présence d'une couche limite de bulles d'air près du fond du canal. On développe une analogie avec les écoulements de solutions diluées de polymers et avec les écoulement diphasiques dans une couche limite. La couche limite de bulles d'air induit une augmentation locale de la viscosité cinématique du fluide près de la paroi, et une expansion de la sous-couche laminaire (viscous sublayer).

L'auteur suggère que cette analogie peut être étendue aux écoulements avec suspension de matériaux, qui sont sujets, aussi, à des réductions du coefficient de frottement.

TABLE OF CONTENTS

NOTATION

The following symbols are used in this report :

B'	integration constant of the equilibrium air concentration distribution;
C	air concentration defined as the volume of air per unit volume;
C_b	air concentration next to the spillway bottom at the outer edge of the air concentration boundary layer;
C_s	mean volumetric sediment concentration;
C_{sb}	volumetric sediment concentration at the outer edge of the viscous sublayer;
C_{mean}	depth averaged air concentration defined as : $(1 - Y_{90}) * C_{mean} = d$;
D_H	hydraulic diameter (m) defined as : $D_H = 4 * \frac{d * W}{W + 2 * d}$
d	characteristic depth (m) defined as : $d = \int_{C=0\%}^{C=90\%} (1 - C) * dy$
d_b	air bubble diameter (m);
d_s	mean sediment particle diameter (m);
Fr	Froude number defined as : $Fr = \frac{q_w}{\sqrt{g * d^3}}$;
f	friction factor of non-aerated flow;
f_e	friction factor for aerated flow;
f_s	friction factor of suspended laden flow;
G'	integration constant of the equilibrium air concentration distribution;
g	gravity constant (m/s^2);
k_s	equivalent uniform sand roughness (m);
n	exponent of the velocity power law;
Q	discharge (m^3/s);

q	discharge per unit width (m^2/s);
Re	Reynolds number defined as : $Re = \rho_W * \frac{U_W * D_H}{\mu_W}$;
Re+	Reynolds number of boundary layer flows : $Re+ = \rho_W * \frac{V_o * Y_o}{\mu_W}$
	Note : for self-aerated flows $Re+ = \rho_W * \frac{V_{90} * Y_{90}}{\mu_W}$
U_W	flow velocity (m/s) : $U_W = q_W/d$;
u_r	bubble rise velocity (m/s);
V	velocity (m/s);
V_o	free stream velocity (m/s) outside of the boundary layer;
V_{90}	characteristic velocity at Y_{90} (m/s);
V_*	shear velocity (m/s);
v'	root mean square of lateral component of turbulent velocity (m/s);
W	channel width (m);
Y_o	boundary layer thickness (m);
Y_{90}	characteristic depth (m) where the air concentration is 90%;
y	distance from the bottom measured perpendicular to the spillway surface (m);
y'	dimensionless depth : $y' = y/Y_{90}$;
α	spillway slope;
Δ_{ab}	dimensionless air concentration boundary layer thickness (m) : $\Delta_{ab} = \rho_W * \frac{\delta_{ab} * V_*}{\mu_W}$
δ_{ab}	air concentration boundary layer thickness (m);
μ	dynamic viscosity ($N.s/m^2$);
ν	kinematic viscosity (m^2/s);
ρ	density (kg/m^3);
σ	surface tension between air and water (N/m).

Subscript

air	air flow;
aw	air-water flow;
s	sediment;
sw	sediment-laden flow;
w	water flow

1. INTRODUCTION

For a spillway flow the upstream flow region is smooth and glassy. Next to the invert turbulence is generated and the boundary layer grows until the outer edge of the boundary layer reaches the surface (fig. 1). From this location, called the point of inception, the turbulent velocity acting next to the free surface can initiate natural free surface aeration. This process is called self-aeration. The boundary layer becomes fully developed and extends up to the free surface. Downstream of the point of inception, a layer containing a mixture of both air and water extends gradually through the fluid. The rate of growth of the layer is small. From the point where the air has reached the chute invert, the air concentration distribution continues to vary gradually with distance. Further downstream the air-water flow becomes uniform.

Self-aeration was studied initially because the entrained air increases the bulk of the flow (FALVEY 1980). Further the presence of air reduces the friction losses (WOOD 1983) and the resulting increase of flow momentum must be taken into account when designing a stilling basin downstream of a spillway. Also the presence of air in high velocity flows may be prevent or reduce the cavitation erosion damage to spillway surfaces (MAY 1987).

In the paper the characteristics of self-aerated flows are summarised in the first part. New results on drag reduction in self-aerated flows are discussed. Model and prototype data are presented. An analogy with dilute polymer solutions, micro-bubble modified boundary layers and sediment laden flows is developed.

Mechanisms of air entrainment

In high speed flows, air entrainment is caused by the turbulent velocity acting next to the air-water interface. Through this interface air is continuously being trapped and released, and the resulting air-water mixture may extend to the spillway invert. Air

entrainment occurs when the turbulence level is large enough to overcome both surface tension and gravity effects : i.e., the turbulent velocity normal to the free surface v' must be large enough to overcome the surface tension pressure (SENE 1984, ERVINE and FALVEY 1987) and greater than the bubble rise velocity component for the bubble to be carried away. These conditions become :

$$v' > \sqrt{\frac{8 * \sigma}{\rho_w * d_b}} \qquad (1)$$

and $v' > u_r * \cos\alpha$ (2)

where σ is the surface tension, ρ_w is the water density, d_b is the air bubble diameter, u_r is the bubble rise velocity and α is the spillway slope. Air entrainment occurs when the turbulent velocity v' satisfies both equations (1) and (2). Assuming a rise velocity of 0.25 m/s, equations (1) and (2) suggest that self-aeration occurs for turbulent velocities normal to the free surface greater than 0.1 to 0.3 m/s, and bubbles in the range 8 to 40 mm are the most likely to be entrained. On prototype spillways the flow conditions are fully turbulent, and the conditions for free surface aeration are always satisfied when the growing boundary layer reaches the free surface. Downstream of the point of inception large quantities of air are entrained and reductions of the friction factor are observed.

Definitions

The local air concentration C is defined as the volume of air per unit volume of air and water. The characteristic flow depth d is defined as :

$$d = \int_0^{Y_{90}} (1 - C) * dy \qquad (3)$$

where y is measured perpendicular to the spillway surface and Y_{90} is the depth where the local air concentration is 90%. The depth averaged mean air concentration C_{mean} is defined as:

$$(1 - C_{mean}) * Y_{90} = d \quad (4)$$

The average water velocity U_W is defined as :

$$U_W = \frac{q_W}{d} \quad (5)$$

where q_W is the water discharge per unit width. The characteristic velocity V_{90} is defined as that at Y_{90}.

2. SELF-AERATED FLOW CHARACTERISTICS

Downstream of the point of inception of air entrainment, the air concentration distributions can be represented by a diffusion model of the air bubbles within the air-water mixture (WOOD 1984) as :

$$C = \frac{B'}{B' + e^{-(G'*\cos\alpha*y'^2)}} \quad (6)$$

where B' and G' are functions of the mean air concentration only and $y' = y/Y_{90}$. Values of B' and G' were computed for STRAUB and ANDERSON's (1958) data. The results are presented in from table I, columns 2 and 3, as functions of the mean air concentration (column 1).

Next to the spillway bottom, the data of CAIN (1978) and CHANSON (1988) depart from equation (6) and indicate that the air concentration tends to zero at the bottom (fig. 2). The existence of an air concentration boundary layer is consistent with the data of BOGDEVICH et al. (1977), MADAVAN et al. (1984) and MARIE et al. (1991) who studied the injection of micro-air-bubbles in turbulent boundary layer flows (table II). Their measurements of air bubble concentration distributions showed also that the bubble concentration falls off to zero at a solid boundary and indicated the presence of an air concentration boundary layer. A re-analysis of the data obtained by BOGDEVICH et al. (1977) and CAIN (1978) shows that the air concentration distribution, in the air concentration boundary layer, may be estimated as :

$$C = C_b * \left(\frac{y}{\delta_{ab}}\right)^{0.270} \qquad (7)$$

where δ_{ab} is the air concentration boundary layer thickness, and C_b is the air concentration at the outer edge of the air concentration boundary layer. C_b satisfies the continuity between equations (6) and (7). If $\delta_{ab} << Y_{90}$, it can be estimated as : $C_b = B'/(B'+1)$ (table I, column 4). Equation (7) is plotted on figure 3 and compared with experimental data.

For the data of BOGDEVICH et al. (1977), CAIN (1978) and CHANSON (1988) data, the dimensionless thickness of the air concentration boundary layer, $\Delta_{ab} = \frac{\delta_{ab} * V_*}{\nu_w}$, is plotted versus the Reynolds number $Re+ = \frac{V_o * Y_o}{\nu_w}$ on figure 4, where V_* is the shear velocity, ν_w is the kinematic viscosity of water, V_o is the velocity outside the boundary layer, Y_o is the boundary layer thickness. For self-aerated flows, V_o and Y_o equal respectively V_{90} and Y_{90}. For the same data, Δ_{ab} is plotted versus the air concentrations C_b on figure 5. It is reasonable to believe that Δ_{ab} does not depend on the air concentration at the outer edge of the air concentration boundary layer. Further the air concentration distribution within the air concentration boundary layer (eq. (7)) is independent of C_b as shown on figure 3.

In self-aerated flows, velocity measurements obtained on a prototype spillway (CAIN 1978) and on a spillway model (CHANSON 1988) indicate that the velocity distribution of the air-water mixture is not affected by the presence of air bubbles. CAIN and WOOD (1981) showed that the velocity distribution can be approximated by :

$$\frac{V}{V_{90}} = \left(\frac{y}{Y_{90}}\right)^{1/n} \qquad (8)$$

where V is the velocity and the exponent n, for the roughness of the Aviemore dam, is : n = 6.0 (CHANSON 1989). On Aviemore dam the non aerated friction factor,

computed from the Colebrook-White formula, is in the range 0.022 to 0.023. Equation (8) was obtained with mean air concentrations in the range 0 to 50 %.

For a given mean air concentration, the characteristic velocity V_{90} can be deduced by combining equations (6), (7) and (8) with the continuity equation for water. Results are given in table I, column 5.

3. DRAG REDUCTION IN SELF-AERATED FLOWS

Presentation

The presence of air bubbles does not affect the velocity distribution but is expected to reduce the shear stress between the flow layers (KILLEN 1968, WOOD 1983, CHANSON 1992a). WOOD (1983) showed that self-aeration induces a drag reduction which increases with the mean air concentration. The author (CHANSON 1992a) re-analysed prototype and model data and the results showed that the drag reduction can be estimated as :

$$\frac{f_e}{f} = 0.307 + 0.1446 * \log_{10}(Re) - 1.4 * C_{mean} \qquad (9)$$

where f is the non-aerated flow friction factor, f_e is the aerated friction factor, $Re = \frac{U_W * D_H}{\nu_W}$ and D_H is the hydraulic diameter. Equation (9) was obtained for $C_{mean} > 0.25$ and Re in the range $2\ 10^5$ to $4\ 10^7$. HARTUNG and SCHEUERLEIN (1970) studied open channel flows on rockfilled channels, with great natural roughness and steep slopes. The extremely rough bottom induced a highly turbulent flow with air entrainment. Their results indicated also a drag reduction due to the presence of air that may be expressed as :

$$\frac{f_e}{f} = \frac{1}{(1 - 3.2 * \sqrt{f} * \log_{10}(1 - C_{mean}))^2} \qquad (10)$$

Drag reduction on prototype spillways

The author re-analysed a new set of prototype data obtained in Australia, Austria, Indonesia, USA, USSR and Yugoslavia (table III) using the method introduced by WOOD (1983) and extended by CHANSON (1992a). For model and prototype data, the drag reduction is estimated as :

$$\frac{f_e}{f} = 0.5 * \left(1 + \tanh\left(0.628 * \frac{0.514 - C_{mean}}{C_{mean} * (1 - C_{mean})}\right)\right) \quad (11)$$

where $\tanh(x) = (e^X - e^{-X}) / (e^X + e^{-X})$. The experimental data are presented in figure 6 and compared with equation (11). For these data the relative roughness k_s/D_H was in the range $3\ 10^{-4}$ up to $4\ 10^{-2}$ and the Reynolds number Re was in the range $5\ 10^4$ to $3\ 10^7$.

Figure 6 indicates that the aerated friction factor f_e departs from the non aerated value f for mean air concentrations larger than 20%. For $C_{mean} > 20\%$ the air concentration next to the chute invert becomes larger than zero, and the air bubbles start interacting with the shear layers next to the invert.

Discussion

An interesting aspect of the drag reduction in self-aerated flows is the interactions between the drag reduction, the velocity profile, and the air concentration distribution next to the chute invert. By analogy with dilute polymer solutions (VIRK 1975, LUMLEY 1977) and microbubble-modified boundary layers (BOGDEVICH et al. 1977, MARIE 1987, MARIE et al. 1991), the air concentration boundary layer might play a role similar to the elastic sub-layer and viscous sublayer in the drag reduction process. The presence of air bubbles next to a solid boundary (e.g. invert, flat plate) increases the effective dynamic viscosity, resulting in a thickening of the viscous sublayer (LUMLEY 1977, MARIE 1987).

MARIE (1987) developed an analytical model to predict the drag reduction due to the presence of air bubbles next to the wall. This model is based on the thickening of the sublayer due to the increase of kinematic viscosity of the air-water flow next to the boundary, compared with a water boundary layer flow. The density of air is 1000 time less than the density of water. In the flow layers close to the boundary, the effective density of the air-water mixture can be approximated as :

$$\rho_{aw} = \rho_w * (1 - C_b) \qquad (12)$$

where ρ_{aw} is the air-water density and C_b is the air concentration at the outer edge of the air concentration boundary layer. EINSTEIN (1906, 1911) proved that the effective viscosity can be estimated as :

$$\mu_{aw} = \mu_w * (1 + 2.5 * C_b) \qquad (13)$$

where μ_{aw} is the effective viscosity of the air-water mixture and μ_w is the water viscosity. Using equations (12) and (13), MARIE's (1987) calculations yield to :

$$\frac{f_e}{f} = \left(1 + \sqrt{\frac{f}{8}} * \left(10.5 * \left(\frac{1+2.5*C_b}{1 - C_b} - 1\right) - 2.44 * \mathrm{Ln}\left(\frac{1+2.5*C_b}{1 - C_b}\right)\right)\right)^{-9/5} \qquad (14)$$

Equation (14) is plotted on figure 6 as a function of the mean air concentration for several values of the non-aerated friction factor, using the air concentration at the outer edge of the air concentration boundary layer C_b deduced from table I (column 4). In the air concentration boundary layer, experimental data (CAIN 1978, CHANSON 1988, 1992b) and calculations (CHANSON 1992c) indicate that, next to the spillway invert, the bubble sizes are small (i.e. d_b < 1 mm). These values are of the same order of magnitude as the experiments of BOGDEVICH et al. (1977) and MADAVAN et al. (1984,1985) used to verify MARIE's (1987) model (table II). Hence it is relevant to compare equations (11) and (14) as shown on figure 7. The agreement between the equations is good and confirms the analogy between the mechanisms of drag reduction.

The author (CHANSON 1992b) suggested that the small air bubbles observed in the air concentration boundary layer act as rigid spheres (COMOLET 1979) and offer a large resistance to break up under the action of turbulent shear stress. It is believed that such rigid air bubbles behave as macro-molecules of polymer and block the turbulence bursting processes in the air concentration boundary layer as macro-molecules do in the viscous sub-layer (VIRK 1975). Further dilute polymer solutions can exhibit macromolecular elongation characteristics that induces an increase of viscosity in the outer region of the sublayer called the elastic sublayer (VIRK 1975, TAM et al. 1992). In self-aerated flows the presence of air bubbles at the outer edge of the air concentration boundary layer is similar to the presence of elongated macromolecules in the elastic sublayer. Air bubbles and elongated macromolecules increase the viscosity and "this increase in viscosity, in the turbulent part and not in the viscous sublayer, suppresses the eddies which carries the Reynolds stress in the buffer layer, resulting in a thickening of the sublayer, and a reduction in drag" (LUMLEY 1977). It must be noted that LUMLEY's conclusion emphasises the significance of the air concentration boundary layer in the drag reduction process taking place in self-aerated flows.

Analogy with suspended sediment flows

In laboratory and river flows, suspended sediment is observed to increase the flow velocity and to decrease the friction factor (BUCKLEY 1923, VANONI 1946, VANONI and NOMICOS 1960, GRAF 1971). Model and prototype data are presented on figure 8 where the friction factor of sediment laden flows is plotted as a function of the mean volumetric sediment concentration C_s, assuming a sediment density of 2500 kg/m^3. Details of the flow conditions are given in table IV. It must be emphasised that the data of BUCKLEY (1923) must be considered with great care as the changes in friction factor due to variation in bed configuration might be important.

Despite earlier controversies in the 1950's and 1960's, it was proved recently that the velocity distribution in the inner flow region follows a logarithmic profile and exhibits a viscous sublayer (COLEMAN 1981, LYNN 1988). Drag reduction in suspended-laden flows is observed with large sediment concentrations. By analogy with air-water flows and dilute polymer solutions, the presence of suspended particles might induce a thickening of the sublayer and a reduction of bottom shear stress. In the flow layers next to the bottom, the presence of sediment increases the density and the viscosity of the flow. At the outer edge of the viscous sublayer, the density of sediment laden flow ρ_{sw} is :

$$\rho_{sw} = \rho_w * \left(1 + C_{sb} * \left(\frac{\rho_s}{\rho_w} - 1\right)\right) \qquad (15)$$

where ρ_s is the sediment density and C_{sb} is the volumetric concentration of sediment at the outer edge of the viscous sublayer. If the suspension is stable, the dynamic viscosity of the sediment-water mixture μ_{sw} can be estimated as (GRAF 1971) :

$$\mu_{sw} = \mu_w * (1 + 2.5 * C_{sb} + (2.5 * C_{sb})^2) \qquad (16)$$

for volume concentrations up to 35 %. Combining equations (15) and (16), the kinematic viscosity of the sediment-water mixture increases with the sediment concentration for $\rho_s/\rho_w < 3.5$. Then MARIE's (1987) model would predict a drag reduction as:

$$\frac{f_s}{f} = \left(1 + \sqrt{\frac{f}{8}} * \left(10.5 * \left(\frac{1 + 2.5*C_{sb} + 6.25*C_{sb}^2}{1 + C_{sb}*\left(\frac{\rho_s}{\rho_w} - 1\right)} - 1\right) - 2.44 * \mathrm{Ln}\left(\frac{1 + 2.5*C_{sb} + 6.25*C_{sb}^2}{1 + C_{sb}*\left(\frac{\rho_s}{\rho_w} - 1\right)}\right)\right)\right)^{-9/5} \qquad (17)$$

where f_s is the friction factor of suspended sediment flows. VANONI (1946), VANONI and NOMICOS (1960) and WANG and QIAN (1989) performed experiments with suspended sediments without depositing material. For these data, equation (17) was computed using the sediment concentration measured at a distance 0.05*d above the

bed. The results are plotted on figure 9 as a function of the observed relative friction factor f_s/f. Equation (17) shows a reasonable agreement with the model data.

By analogy with air-water shear flows and dilute polymer solutions, an increase of viscosity in the flow layers next to the boundary might explain the observed drag reduction in suspended particle flows. But it must be emphasised that the sediment concentration increases toward a maximum at the channel bottom and no concentration boundary layer is observed. Further LYN (1991) highlighted the importance of the ratio of the sublayer thickness over the flow depth and suggested an increase of friction factor for sediment laden flows in shallow waters and for small sediment concentrations.

4. CONCLUSION

The characteristics of self-aerated flows are summarised for chute spillways. In particular self-aeration induces a substantial reduction of the friction factor on both models and prototypes. Although the velocity distribution is not affected by the presence of air bubbles, the shape of the air concentration distribution shows the presence of an air concentration boundary layer that plays a major role in the drag reduction process. By analogy with dilute polymer solutions and microbubble modified boundary layers, it is suggested that the presence of air next to the invert increases the effective viscosity of the mixture and the sublayer thickness, and induces drag reduction as observed on prototype (fig. 6).

A similar mechanism might explain also the drag reduction observed in sediment laden flows. But at the present time, insufficient prototype data are available and additional work on the interactions between the velocity distribution and sediment concentration distribution is required.

REFERENCES

AIVAZYAN, O.M. (1986). "Stabilized Aeration on Chutes." *Gidrotekhnicheskoe Stroitel'stvo*, No. 12, pp. 33-40 (Hydrotechnical Construction, 1987, Plenum Publ., pp. 713-722).

BOGDEVICH, V.G., EVSEEV, A.R., MLYUGA, A.G., and MIGIRENKO, G.S. (1977). "Gas-Saturation Effect on Near-Wall Turbulence Characteristics." *Proc. of the 2nd Intl. Conf. on Drag Reduction*, BHRA Fluid Eng., Cambridge, UK, Paper D2, pp. 25-37.

BUCKLEY, A.B. (1923) "The Influence of Silt on the Velocity of Water Flowing in Open Channels." *Minutes of the Proc. Instn Civ. Engrs.*, 1922-1923, Vol. 216, Part II, pp. 183-211. Discussion, pp. 212-298.

CAIN, P. (1978). "Measurements within Self-Aerated Flow on a Large Spillway." *Ph.D. Thesis*, Ref. 78-18, 1978, Univ. of Canterbury, Christchurch, New Zealand.

CAIN, P., and WOOD, I.R. (1981). "Measurements of Self-aerated Flow on a Spillway." *Jl. Hyd. Div.*, ASCE, 107, HY11, pp. 1425-1444.

CHANSON, H. (1988). "A Study of Air Entrainment and Aeration Devices on a Spillway Model." *Research Rep. 88-8*, Oct., Univ. of Canterbury, New Zealand.

CHANSON, H. (1989). "Flow downstream of an Aerator. Aerator Spacing." *Jl of Hyd. Research*, IAHR, Vol. 27, No. 4, pp. 519-536.

CHANSON, H. (1992a). "Entraînement d'Air dans les Ecoulements à Surface Libre : Application aux Evacuateurs de Crues de Barrage. " ('Air Entrainment in Open Channel Flow : Application to Spillways.') *Jl 'La Houille Blanche'*, No. 4, 1992, pp. 277-286 (in French).

CHANSON, H. (1992b). "Discussion of 'A General Correlation for Turbulent Velocity Profiles of Dilute Polymer Solutions', by K.C. TAM, C. TIU, and R.J. KELLER, Jl of Hyd. Res., IAHR, Vol. 30, No. 1, 1992, pp. 117-142." *Jl of Hyd. Res.*, IAHR, Vol. 30, No. 6.

CHANSON, H. (1992c). "Air Entrainment in Chutes and Spillways." *Research Report No. CE 133*, Dept. of Civil Engineering, University of Queensland, Australia, Feb., 85 pages.

COLEMAN, N.L. (1981). "Velocity Profiles with Suspended Sediment." *Jl. of Hyd. Res.*, IAHR, Vol. 19, No. 3, pp. 211-229.

COMOLET, R. (1979). "Sur le Mouvement d'une bulle de gaz dans un liquide." ('Gas bubble motion in a liquid medium') *Jl La Houille Blanche*, 1979, No. 1, pp. 31-42 (in French).

EHRENBERGER, R. (1926). "Wasserbewegung in steilen Rinnen (Susstennen) mit besonderer Berucksichtigung der Selbstbelüftung." ('Flow of Water in Steep Chutes with Special Reference to Self-aeration.') *Zeitschrift des Österreichischer Ingenieur und Architektverein*, No. 15/16 and 17/18 (in German) (translated by Wilsey, E.F., U.S. Bureau of Reclamation).

EINSTEIN, A. (1906). "Eine Neue Bestimmung der Moleküldimensionen." *Ann. Phys.*, 19, p. 289.

EINSTEIN, A. (1911). "Eine Neue Bestimmung der Moleküldimensionen." *Ann. Phys.*, 34, p. 591.

ERVINE, D.A., and FALVEY, H.T. (1987). "Behaviour of Turbulent Water Jets in the Atmosphere and in Plunge Pools." *Proc. Instn Civ. Engrs.*, Part 2, Mar. 1987, 83, pp. 295-314.

FALVEY, H.T. (1980). "Air-Water Flow in Hydraulic Structures." *USBR Engrg. Monograph*, No. 41, Denver, Colorado, USA.

GRAF, W.H. (1971). "Hydraulics of Sediment Transport". *McGraw-Hill*, New York, USA.

HALL, L.S. (1943). "Open Channel Flow at High Velocities." *Trans. ASCE*, Vol. 108, pp. 1394-1434.

HARTUNG, F., and SCHEUERLEIN, H. (1970). "Design of Overflow Rockfill Dams." *10th ICOLD Congress*, Montréal, Canada, Q. 36, R. 35, pp. 587-598.

INNEREBNER, K. (1924). "Overflow Channels from Surge Tanks." *World Power Conference*, 1st, Vol. 2, pp. 481-486.

JEVDJEVICH, V., and LEVIN, L. (1953). "Entrainment of Air in flowing Water and Technical Problems connected with it." *Proc. of 5th I.A.H.R. Congress*, IAHR-ASCE, Minneapolis, USA, pp. 439-454.

KILLEN, J.M. (1968). "The Surface Characteristics of Self-Aerated Flow in Steep Channels." *Ph.D. thesis*, University of Minnesota, Minneapolis, USA.

LEVIN, L. (1955). "Quelques Réflexions sur la Mécanique de l'écoulement des Mélanges d'Eau et d'Air." ('Notes on the Flow Mechanics of Water-Air Mixtures.') *Jl La Houille Blanche*, No. 4, Aug.-Sept., 1955, pp. 55-557 (in French).

LUMLEY, J.L. (1977). "Drag Reduction in Two Phase and Polymer Flows." *Physics Fluids*, Vol. 20, No. 10, Pt II, pp. S64-S71.

LYN, D.A. (1988). "A Similarity Approach to Turbulent Sediment-Laden Flows in Open Channels." *Jl Fluid Mech.*, Vol. 193, pp. 1-26.

LYN, D.A. (1991). "Resistance in Flat-Bed Sediment-Laden Flows." *Jl of Hyd. Engrg.*, ASCE, Vol. 117, No. 1, pp. 94-114.

MADAVAN, N.K., DEUTSCH, S., and MERKLE, C.L. (1984). "Reduction of Turbulent Skin Friction by Microbubbles." *Physics Fluids*, Vol. 27, No. 2, pp. 356-363.

MADAVAN, N.K., DEUTSCH, S., and MERKLE, C.L. (1985). "Measurements of Local Skin Friction in a Microbubble-Modified Turbulent Boundary Layer." *Jl Fluid Mech.*, Vol. 156, pp. 237-256.

MARIE, J.L. (1987). "A Simple Analytical Formulation for Microbubble Drag Reduction." *PCH*, Vol. 8, No. 2, pp. 213-220.

MARIE, J.L., MOURSALI, E., and LANCE, M. (1991). "A First Investigation of a Bubbly Boundary Layer on a Flat Plate : Phase Distribution and Wall Shear Stress

Measurements." *Proc. of the 1st ASME-JSME Fluids Eng. Conf.*, Turbulence Modification in Multiphase Flows 1991, June, Portland, USA, FED-Vol. 110, ASME, pp. 75-80.

MAY, R.W.P. (1987). "Cavitation in Hydraulic Structures : Occurrence and Prevention." *Hydraulics Research Report*, No. SR 79, Wallingford, UK.

MICHELS, V., and LOVELY, M. (1953). "Some Prototype Observations of Air Entrained Flow." *Proc. of 5th I.A.H.R. Congress*, AIHR-ASCE, Minneapolis, USA, pp. 403-414.

SENE, K.J. (1984). "Aspects of Bubbly Two-Phase Flow." *Ph.D. thesis*, Trinity College, Cambridge, UK, Dec..

SIMONS, D.B., and RICHARDSON, A.M. (1960). "Resistance Properties of Sediment-Laden Streams. Discussion" *Trans. ASCE*, Vol. 125, Part I, pp. 1170--1172.

STEWART, W.G. (1913). "The Determination of the N in Kutter's Formula for Various Canals, Flumes and Chutes on the Boise Project and Vicinity." *Report on 2nd Annual Conf. on Operating Men*, USBR, Boise, Idaho, USA, Jan., pp. 8-23.

STRAUB, L.G., and ANDERSON, A.G. (1958). "Experiments on Self-Aerated Flow in Open Channels." *Jl of Hyd. Div.*, Proc. ASCE, Vol. 84, No. HY7, paper 1890.

TAM, K.C., TIU, C., and KELLER, R.J. (1992). "A General Correlation for Turbulent Velocity Profiles of Dilute Polymer Solutions." *Jl of Hyd. Res.*, IAHR, Vol. 30, No. 1, pp. 117-142

VANONI, V.A. (1946). "Transportation of suspended sediment in water." *Trans. ASCE*, Vol. 111, pp. 67-133.

VANONI, V.A., and NOMICOS, G.N. (1960). "Resistance Properties of Sediment-Laden Streams." *Trans. ASCE*, Vol. 125, Part I, pp. 1140-1167.

VIRK, P.S. (1975). "Drag Reduction Fundamentals." *AIChE Jl*, Vol. 21, No. 4, pp. 625-656.

WANG, Xingkui, and QIAN, Ning (1989). "Turbulence Characteristics of Sediment-Laden Flow." *Jl of Hyd. Engrg.*, ASCE, Vol. 115, No. 6, pp. 781-800.

WOOD, I.R. (1983). "Uniform Region of Self-Aerated Flow." *Jl Hyd. Eng.*, ASCE, Vol. 109, No. 3, pp. 447-461.

WOOD, I.R. (1984). "Air Entrainment in High Speed Flows." *Proc. of the Intl. Symp. on Scale Effects in Modelling Hydraulic Structures*, IAHR, Esslingen, Germany, H. KOBUS editor, paper 4.1.

Table I - Air concentration and velocity distribution parameters in self-aerated flows

C_{mean}	$G'*\cos\alpha$ [a]	B' [a]	C_b [b]	$\frac{V_{90} * Y_{90}}{q_w}$	f_e/f Eq. (11)
(1)	(2)	(3)	(4)	(5)	(6)
0.0	+ infinite	0.00	0.00	1.167	1.0
0.161	7.999	0.003021	0.02	1.453	0.964
0.241	5.744	0.028798	0.04	1.641	0.867
0.310	4.834	0.07157	0.07	1.805	0.768
0.410	3.825	0.19635	0.17	2.141	0.632
0.569	2.675	0.62026	0.36	2.985	0.430
0.622	2.401	0.8157	0.46	3.319	0.360
0.680	1.8942	1.3539	0.55	4.151	0.277
0.721	1.5744	1.8641	0.64	4.859	0.215

Note : [a] computed from STRAUB and ANDERSON's (1958) data

[b] computed from equation (6) : $C_b = B'/(B'+1)$

Table II - Drag reduction experiments and air concentration boundary layer characteristics

Reference	δ_{ab} mm	Bubble size d_b mm	C_b	Velocity V_o m/s	Comments
(1)	(2)	(3)	(4)	(5)	(6)
BOGDEVICH et al. (1977)	0.7 to 3.4	0.002 to 0.1	0.14 to 0.7	4.3 to 10.9	Microbubble-modified boundary layer.
MADAVAN et al. (1984)		0.005		4 to 17	Microbubble-modified boundary layer.
MADAVAN et al. (1985)		0.0005 to 0.1		4 to 17	Microbubble-modified boundary layer.
MARIE et al. (1991)	2	4	0.02 to 0.07	0.5 to 1	Bubbly boundary layer on a flat plate.
CAIN (1978)	10 to 30	0.5 to 5	0.04 to 0.27	18 to 22	Self-aerated flows. Prototype spillway.
CHANSON (1988)	15 to 23	0.3 to 4	0.15 to 0.27	9 to 17	Self-aerated flows. Spillway model.

Notes :

δ_{ab} air concentration boundary layer thickness

C_b air concentration at the outer edge of the air concentration boundary layer

V_o velocity outside the boundary layer

Table III - Self-aerated flow measurements on prototype and model spillways

Spillway	Slope degrees	q_W m^2/s	k_S/D_H	Re	Ref.	Comments
(1)	(2)	(3)	(5)	(6)	(7)	(8)
Prototype	spillway					
Ak-Tepe, USSR	21.8	2.3 to 8.0	5E-3 to 1E-2	8.8E+6 to 2.8E+7	[A]	Rough concrete. W = 5 m. k_S = 5 mm.
Aviemore, New Zealand	45.0	2.23 & 3.16	8E-4 to 1.9E-3	8.9E+6 to 1.3E+7	[CA]	Concrete. k_S = 1 mm.
Bencok, Indonesia	31.05	2.9 to 6.0	3E-3 to 4.6E-3	9E+6 to 1.6E+7	[A,E,L]	W = 1 m. k_S = 2 mm.
Big Hill, Australia	4.2	0.74 to 0.82	6.5E-3	2E+6	[M]	Smooth concrete.
Boise, USA	4.6 to 12.2	0.01 to 0.8	2.7E-3 to 3.1E-2	5.3E+4 to 2.8E+6	[S]	Concrete. W = 0.9 to 1.8 m. k_S = 1 mm.
Dago, Indonesia	13.8	0.74 to 1.39	2.5E-3 to 3.4E-3	2.5E+6 to 4.5E+6	[A,E,L]	W = 1 m. k_S = 1 mm.
Erevan, USSR	21.8	0.38 to 1.55	1.9E-2 to 4E-2	1.5E+6 to 5.8E+6	[A]	Rough basalt & cement mortar.W=4 m. k_S=10 mm.
Gizel'don, USSR	28.1	0.49 to 1.28	5E-4 to 1.1E-3	1.9E+6 to 5E+6	[A]	Wooden flume. W = 6 m. k_S = 0.3 mm.
Hat Creek, USA	23.45 to 34.75	1.86 to 6.4	4.8E-3 to 1.2E-2	6E+6 to 2E+7	[H]	Rough concrete. W = 1.75 m. k_S = 5 mm.
Kittitas, USA	33.2	2.24 to 11.7	7E-3 to 2E-2	8E+6 to 3E+7	[H]	Eroded concrete. W = 2.44 m. k_S = 10 mm.
Mallnitz, Austria	22.2				[A,E,L]	Concrete. W = 2m.
Mostarsko Blato, Yugoslavia		0.71 to 3.44	1.5E-2 to 3.5E-2	8.3E+4 to 3E+7	[J]	Stone lining. W = 5.35 m. k_S = 20 mm.
Rapid Flume, USA	20.1	1.76	3E-4	6E+6	[H]	Wooden flume. W = 1.4 m. k_S = 0.1 mm.
Spring Gully, Australia	5.3		6E-3 to 7E-4	2E+6	[M]	Smooth concrete. Semi circular (R=0.61 m).
Rutz, Austria	34	0.4 to 2	3E-4 to 1.3E-3	2E+6 to 7E+6	[I]	Concrete. Trapezoidal.
Spillway	models					
Clyde model, New Zealand	52.3	0.21 to 0.48	3.8E-4 to 1.2E-3	8E+5 to 2E+6	[CH]	Perspex. D/S of aerator. W=0.25 m. k_S=0.1 mm.
IWP, USSR	16.7 & 29.7	0.064 to 0.13	1.3E-3 to 2.6E-3	2.3E+5 to 4.3E+5	[A]	Planed board with painting. W=0.25 m. k_S=0.1 mm.
Vienna Lab., Austria	8.7 to 31.2	0.04 to 0.178			[A,E,J,L]	Wooden flume. W=0.25 m.
St Anthony Falls, USA	7.5 to 75	0.14 to 0.93	3E-3 to 1.6E-2	4.7E+5 to 2E+6	[SA]	Artificial roughness. W=0.46 m. k_S=0.7 mm.
Rockfilled	channels					
Obernach, Germany	6 to 34		0.02 to 0.2		[HS]	k_S = 0.1 to 0.35 m.

Notes for table III :

[A] AIVAZYAN (1986); [CA] CAIN (1978); [CH] CHANSON (1988); [E] EHRENBERGER (1926); [H] HALL (1943); [HS] HARTUNG and SCHEUERLEIN (1970); [I] INNEREBNER (1924); [J] JEVDJEVICH and LEVIN (1953) [L] LEVIN (1955); [M] MICHELS and LOVELY (1953); [S] STEWART (1913); [SA] STRAUB and ANDERSON (1958).

Table IV - Suspended sediment flow measurements on models and prototypes

Reference	Discharge m^3/s	C_S	U_W m/s	Comments
(1)	(2)	(3)	(4)	(5)
BUCKLEY (1923)	900 to 6700	120 to 1,620 g/m^3	0.5 to 1.4	Prototype data. Nile river at Beleida discharge station.
	47 to 68	14 to 2,050 g/m^3	0.52 to 0.68	Prototype data. Canal derivation from the Nile river.
VANONI (1946)	0.03 to 0.15	0 to 3,190 g/m^3	0.55 to 1.2	Model data. W = 0.84 m.
VANONI and NOMICOS (1960)	0.014	0 to 8,100 g/m^3	0.69 to 0.70	Model data. W = 0.27 m.
SIMONS and RICHARDSON (1960)		40,000 ppm		Fine sediments (clays).
WANG and QIAN (1989)	0.044 to 0.06	0 to 2.1%	1.9	Beach sand in clear water flow. ρ_S = 2640 kg/m^3. d_S = 0.15 mm.

Notes :

C_S average sediment concentration

d_S mean particle size

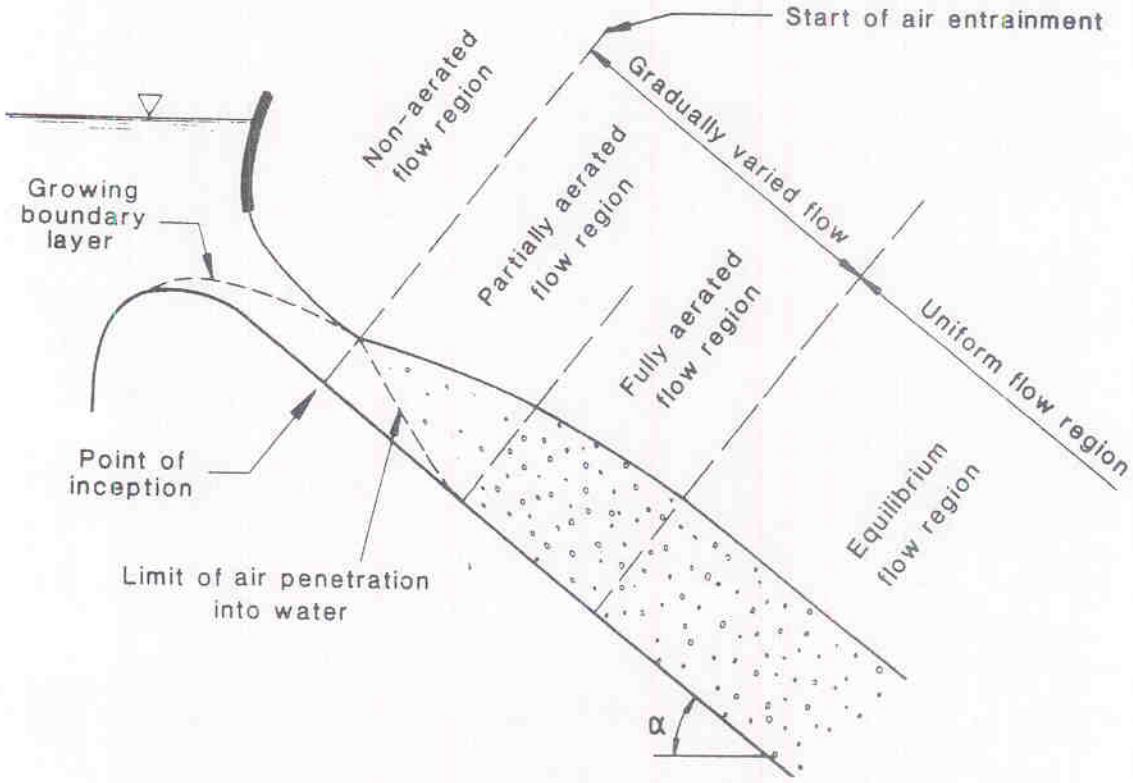

Fig. 1 - Air entrainment along a spillway

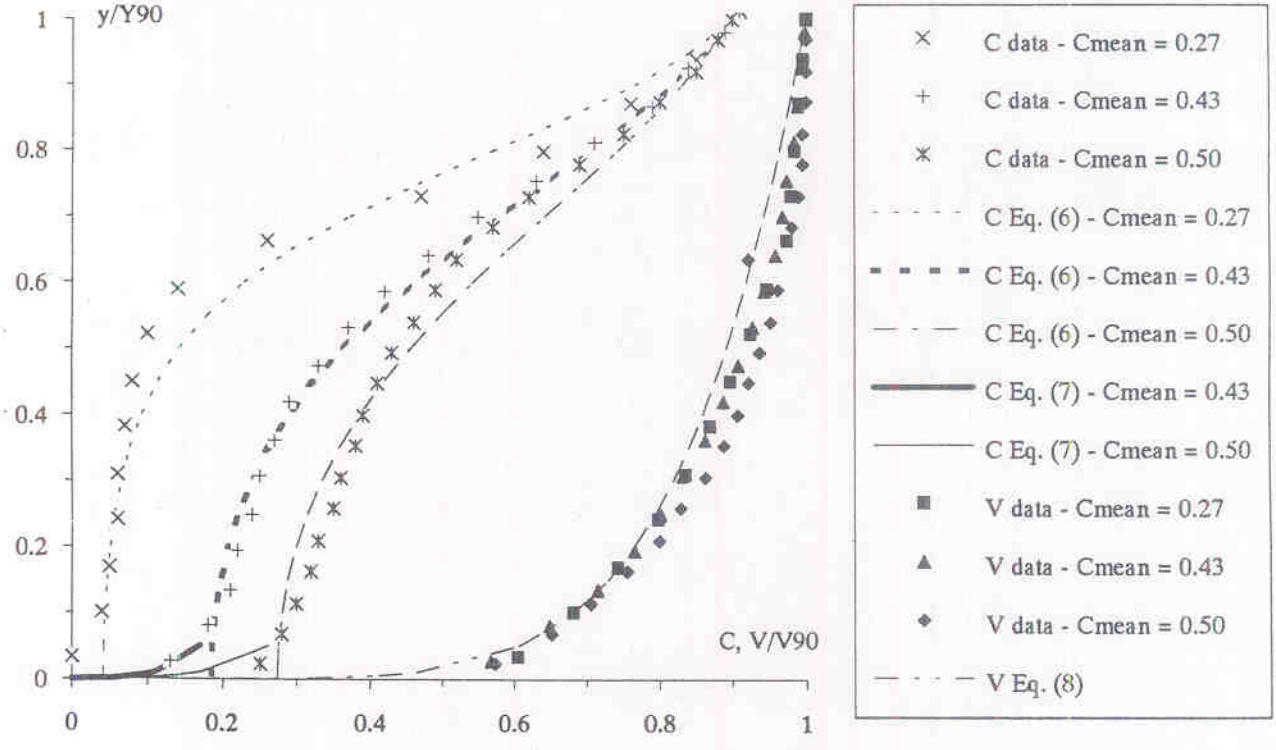

Fig. 2 - Air concentration and velocity distributions at Aviemore spillway (CAIN 1978)

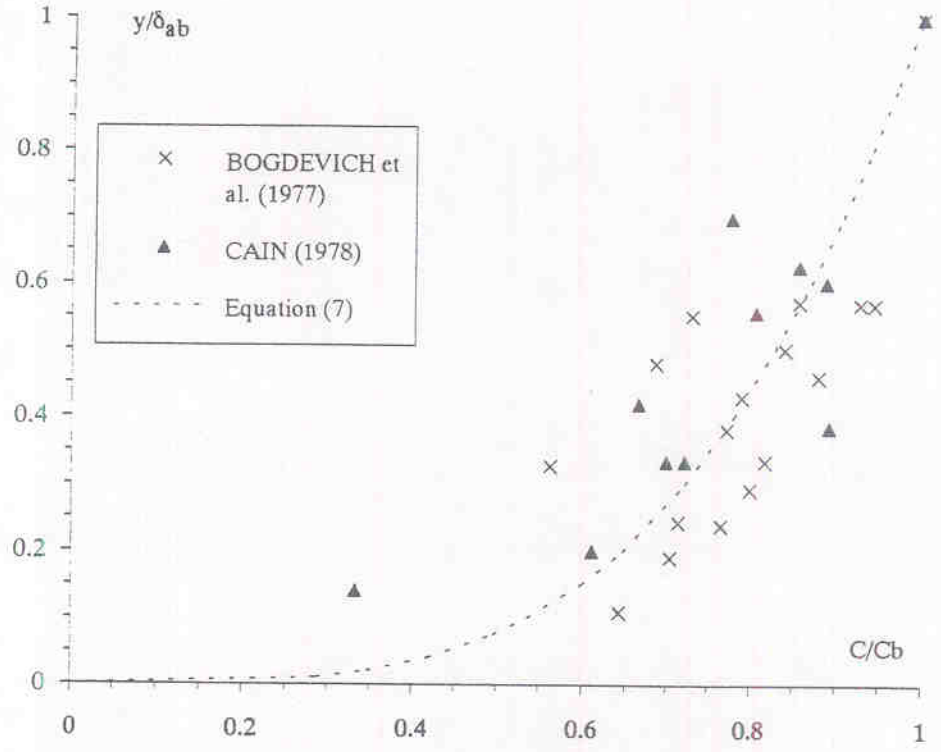

Fig. 3 - Air concentration distribution in the air concentration boundary layer

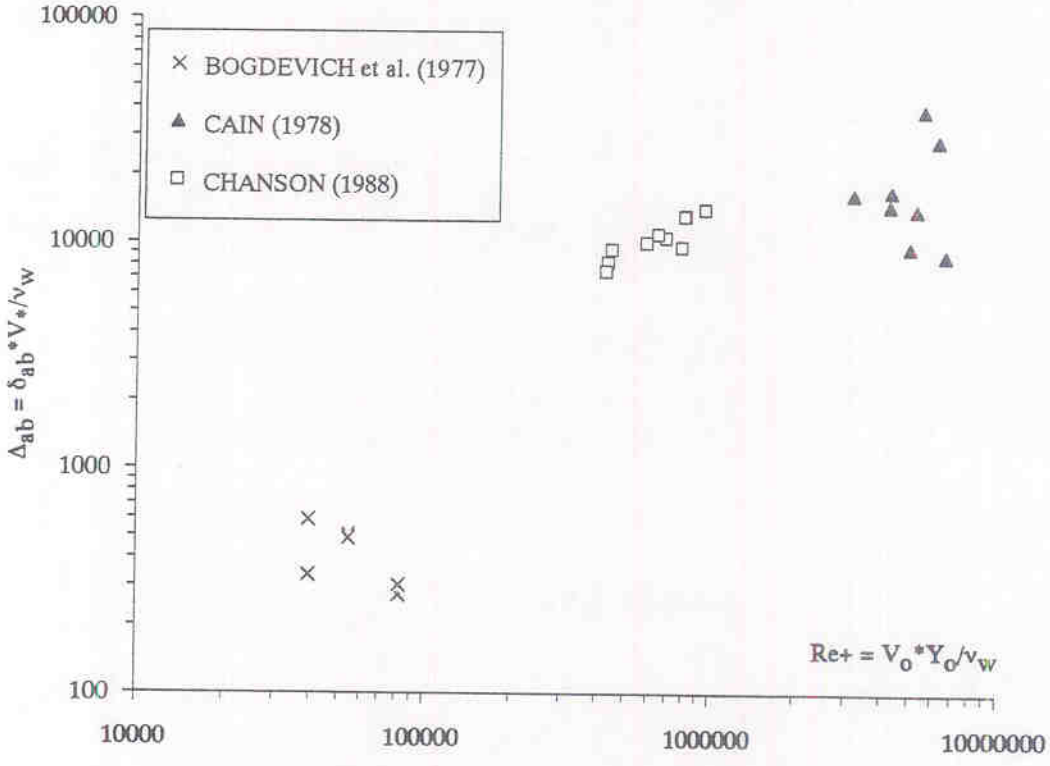

Fig. 4 - Dimensionless thickness of the air concentration boundary layer Δ_{ab} as a function of the Reynolds number Re+

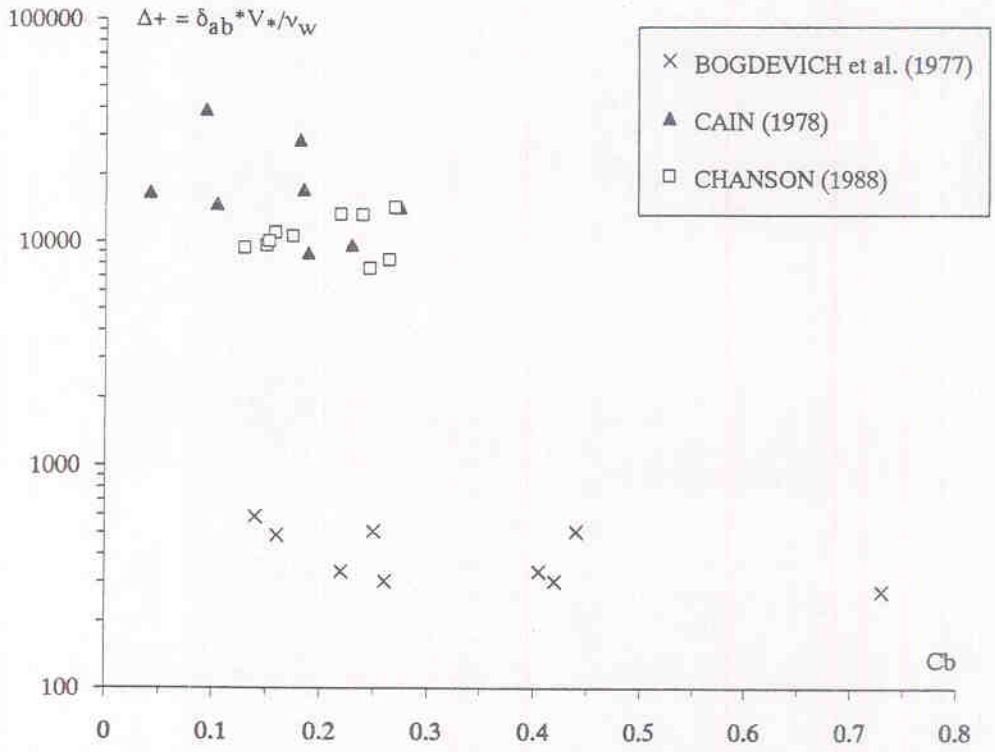

Fig. 5 - Dimensionless thickness of the air concentration boundary layer as a function of the air concentration at the outer edge of the air concentration boundary layer C_b

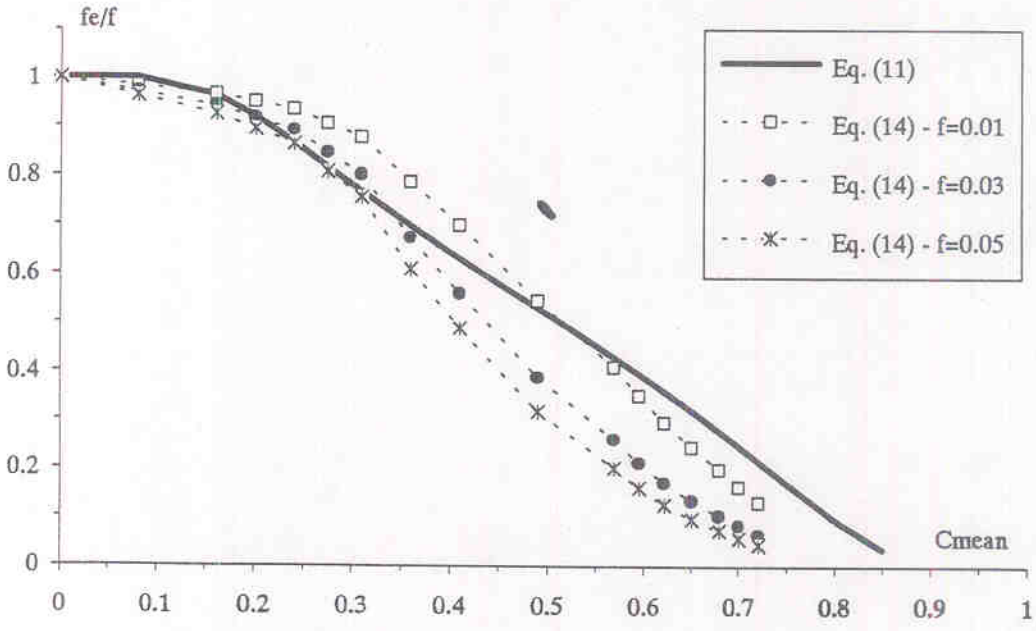

Fig. 7 - Drag reduction : comparison between equations (11) and (14)

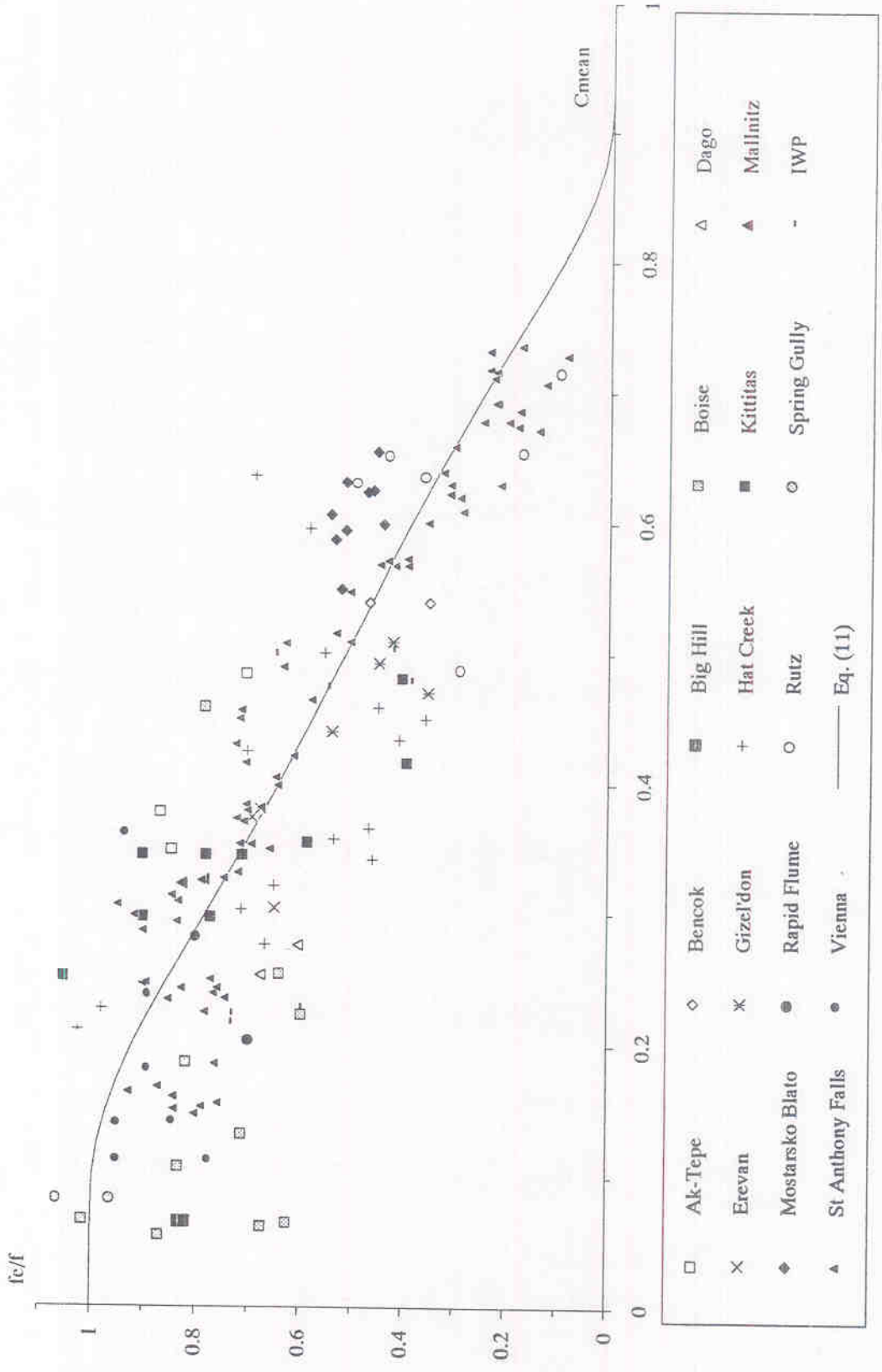

Fig. 6 - Drag reduction observed on prototype spillways and spillway models

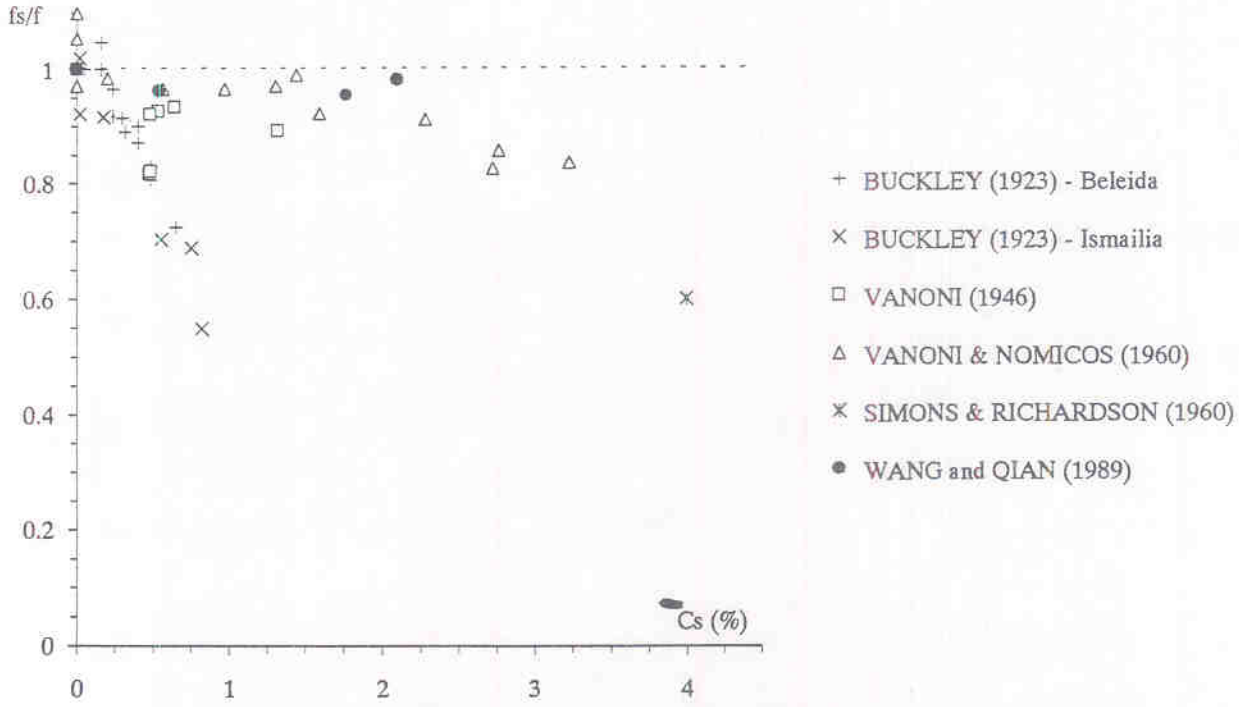

Fig. 8 - Drag reduction observed in sediment laden flows - BUCKLEY (1923), VANONI (1946), VANONI and NOMICOS (1960), SIMONS and RICHARDSON (1960)

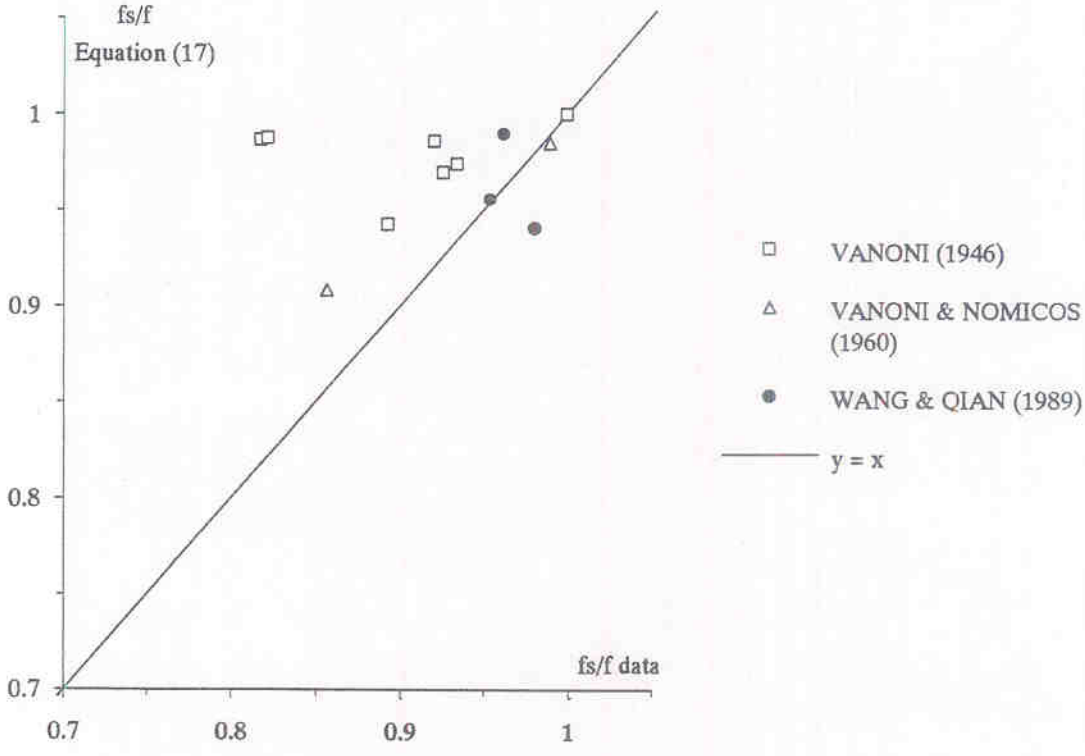

Fig. 9 - Comparison between equation (17) and experimental data